This is a repository copy of *The flavodoxin FldA activates the class Ia ribonucleotide reductase of Campylobacter jejuni*.

White Rose Research Online URL for this paper:
https://eprints.whiterose.ac.uk/173101/

Version: Published Version

RESEARCH ARTICLE

WILEY

The flavodoxin FldA activates the class Ia ribonucleotide reductase of *Campylobacter jejuni*

Abdulmajeed Alqurashi[1] | Laura Alfs[2] | Jordan Swann[2] | Julea N. Butt[2] |
David J. Kelly [iD] [1]

[1]Department of Molecular Biology and Biotechnology, The University of Sheffield, Sheffield, UK

[2]School of Chemistry, University of East Anglia, Norwich, UK

Correspondence
David J. Kelly, Department of Molecular Biology and Biotechnology, The University of Sheffield, Firth Court, Western Bank, Sheffield S10 2TN, UK.
Email: d.kelly@sheffield.ac.uk

Abstract

Campylobacter jejuni is a microaerophilic zoonotic pathogen with an atypical respiratory Complex I that oxidizes a flavodoxin (FldA) instead of NADH. FldA is essential for viability and is reduced via pyruvate and 2-oxoglutarate oxidoreductases (POR/OOR). Here, we show that FldA can also be reduced by FqrB (Cj0559), an NADPH:FldA reductase. An *fqrB* deletion mutant was viable but displayed a significant growth defect. FqrB is related to flavoprotein reductases from Gram-positive bacteria that can reduce NrdI, a specialized flavodoxin that is needed for tyrosyl radical formation in NrdF, the beta subunit of class 1b-type (Mn) ribonucleotide reductase (RNR). However, *C. jejuni* possesses a single class Ia-type (Fe) RNR (NrdAB) that would be expected to be ferredoxin dependent. We show that CjFldA is an unusually high potential flavodoxin unrelated to NrdI, yet growth of the *fqrB* mutant, but not the wild-type or a complemented strain, was stimulated by low deoxyribonucleoside (dRNS) concentrations, suggesting FldA links FqrB and RNR activity. Using purified proteins, we confirmed the NrdB tyrosyl radical could be regenerated in an NADPH, FqrB, and FldA dependent manner, as evidenced by both optical and electron paramagnetic resonance (EPR) spectroscopy. Thus, FldA activates RNR in *C. jejuni*, partly explaining its essentiality.

KEYWORDS
Cj0559, flavin, flavodoxin reductase, FqrB, tyrosyl radical

1 | INTRODUCTION

Campylobacteriosis is the most common food-borne bacterial zoonosis worldwide, resulting in a huge public health and economic burden, with *Campylobacter jejuni*, as the major causative agent. Undercooked chicken is the main source of human campylobacteriosis in many countries; 60%–80% of cases may be attributable to poulty reservoirs (Sheppard et al., 2009). However, campylobacters are also found in other farm animals and the environment (e.g., water

sources) with both host/source-specific and generalist strains capable of rapid transition between the different physical, nutritional, and immunological niches of each host or environment. In humans, *C. jejuni* is an intestinal mucosal pathogen that causes an acute bloody diarrhea, severe abdominal cramping, and fever, with ~0.1% of infections leading to transient paralysis (and occasional deaths) due to inflammatory neuropathies (e.g., Guillain–Barré syndrome). In addition, antimicrobial resistance is a major problem, with an increasing prevalence of fluoroquinolone resistance in particular

(Haldenby et al., 2020), and *C. jejuni* has been designated a World Health Organization (WHO) priority organism for developing novel antimicrobial agents. New insights into *C. jejuni* biology are needed if control measures are to be put in place that more effectively reduce chicken colonization and/or food-chain contamination.

C. jejuni is a microaerophile, adapted for growth at low oxygen niches in the host, with most strains unable to grow at atmospheric oxygen levels. Compared with conventional aerobes, *C. jejuni* is unique in utilizing oxidant-labile enzymes in central metabolic pathways, which are critical for growth (Kendall et al., 2014). In particular, it employs pyruvate and 2-oxoglutarate: acceptor oxidoreductases (POR and OOR), rather than oxygen-stable NAD-linked 2-oxoacid dehydrogenases, to transfer substrate-derived electrons to the respiratory chain (Taylor & Kelly, 2019; Weerakoon & Olson, 2008). These enzymes contain Fe–S clusters vulnerable to oxidative damage; we have previously shown that exposure of *C. jejuni* cells to prolonged aeration causes their inactivation in vivo, which may be a major contributor to the microaerophilic phenotype (Kendall et al., 2014). Conversely, we could not demonstrate consistent growth under strictly anaerobic conditions, even in the presence of alternative electron acceptors that do allow growth under oxygen-limiting conditions (Sellars et al., 2002). This seems to be due to the presence of a single class Ia-type ribonucleotide reductase (RNR) that would require catalytic amounts of oxygen to sustain DNA synthesis.

The electron acceptor for OOR has been shown to be the flavodoxin FldA (Cj1382; CjFldA), which has a flavin mononucleotide (FMN) cofactor. FldA is the sole flavodoxin encoded in the genome of *C. jejuni* NCTC 11168 (Parkhill et al., 2000; Weerakoon & Olson, 2008). Reduced FldA is thought to be reoxidized by donation of electrons from FMN to the membrane bound Complex I of the respiratory chain. In the canonical Complex I found in well studied "model" bacteria, the *nuoE* and *nuoF* genes encode an NADH-binding module that delivers electrons to Fe–S centers in the NuoG subunit. However, in *C. jejuni*, these genes are replaced by two novel genes *cj1575c* (*nuoX*) and *cj1574c* (*nuoY*), the function of which are unknown (Calderon-Gomez et al., 2017; Smith et al., 2000). Conceivably, they may form a docking site for reduced FldA to deliver electrons to the Fe–S clusters of NuoG (Taylor & Kelly, 2019; Weerakoon & Olson, 2008) but may also have roles independent of Complex I, as unlike all of the other *nuo* genes in *C. jejuni*, *nuoY* (and probably *nuoX*) cannot be deleted (Weerakoon & Olson, 2008). It has also not been possible to delete the *fldA* gene, suggesting that CjFldA must have essential functions (Weerakoon & Olson, 2008). Apart from allowing acetyl-CoA synthesis via POR, one additional likely vital role is in isoprenoid biosynthesis via the methyl erythritol phosphate (MEP) pathway (Heuston et al., 2012). IspG and IspH are 4Fe-4S enzymes that catalyse the last two steps in the formation of the isoprenoid precursors isopentyl pyrophosphate (IPP) and dimethylallyl pyrophosphate (DMAPP); in other bacteria, both reactions require reduced flavodoxin as the electron donor (Puan et al., 2005; Rohdich et al., 2003).

A study in the closely related *Helicobacter pylori* (St Maurice et al., 2007) reported that a flavin adenine dinucleotide (FAD) containing and NADPH oxidizing enzyme named FqrB (HP1164) could also act as a flavodoxin reductase in addition to POR. However, based on in vitro studies, these authors proposed that the physiological function of FqrB was in the production of NADPH via the reversed reaction, that is, the transfer of electrons from pyruvate to NADPH via POR, flavodoxin and FrqB. In *H. pylori*, FqrB is seemingly an essential enzyme as attempts to produce an *fqrB* deletion mutant were unsuccessful (St Maurice et al., 2007). A homologue of FqrB (Cj0559) is also present in *C. jejuni*. Here, we show that CjFldA is an unusually high-potential flavodoxin, making NADP reduction unfavorable. Instead, we demonstrate that FqrB provides an additional route for flavodoxin reduction using NADPH as the ultimate electron donor and that both FqrB and FldA are involved in tyrosine radical formation in, and thus activation of, the *C. jejuni* RNR.

2 | RESULTS

2.1 | Redox properties of the *C. jejuni* flavodoxin: CjFldA is an unusually high redox potential flavodoxin that can be reduced by both POR and OOR

The *C. jejuni* FldA was overproduced in *Escherichia coli* as a C-terminally his-tagged protein and purified by nickel-affinity and hydrophobic interaction chromatography (HIC) (Figure S1a). The as-purified (oxidized) protein has a typical flavodoxin absorption spectrum (Figure 1a; raw data for all figures in Table S1) with maxima at ~380 and ~460 nm that matched those of a previous study reporting the purification of this protein (Weerakoon & Olson, 2008). The semireduced protein displays a shift of the 380 peak to 360 nm and broad absorbance maxima at ~460 and ~600 nm, which are characteristics of neutral semiquinone (Figure 1a). The latter was exploited in optically monitored potentiometric titrations (Figure 1b), to define the flavodoxin reduction potentials at pH 7 of −170 mV versus standard hydrogen electrode (SHE) for the oxidized-semiquinone transition (Q/SQ or E_2) and −190 mV versus SHE for the semiquinone-hydroquinone transition (SQ/HQ or E_1).

Independent assessment of the redox properties of CjFldA was afforded by cyclic voltammetry, a powerful electrochemical method to analyze the current response of a redox species with a linearly cycled potential (Figure 1c). For these experiments, the flavodoxin was deposited onto the surface of a pyrolytic graphite edge electrode coated with the surfactant didodecyldimethylammonium bromide (DDAB) (Rusling, 1998; Seagel et al., 2017). Cyclic voltammetry revealed two redox processes. The lower potential process had a mid-point potential of approximately − 250 mV, whereas the higher potential process had a mid-point potential of approximately −150 mV. Neither process was present in voltammetry of DDAB-coated electrodes that had not been exposed to flavodoxin (Figure 1c). Thus, we assign the processes observed with the CjFldA
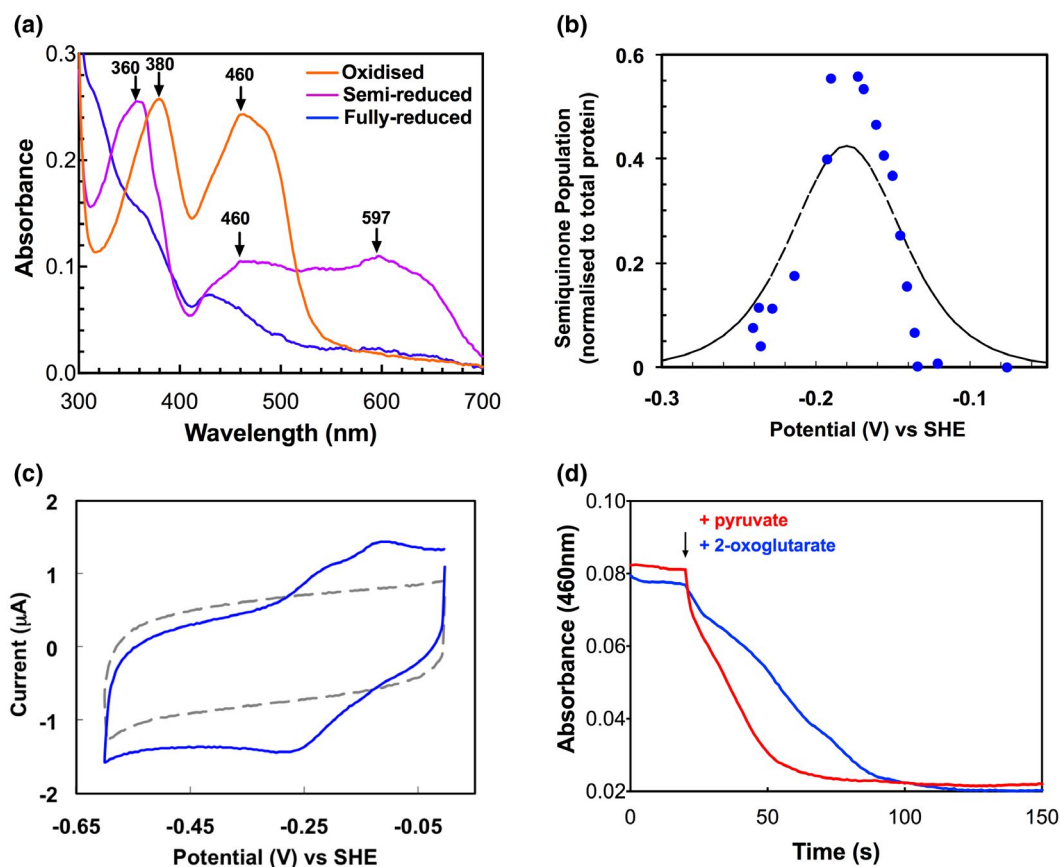
FIGURE 1 Redox properties of the *C. jejuni* flavodoxin FldA. (a) The electronic absorption spectra of the fully oxidized (orange), semi-reduced (purple) and fully reduced (blue) states of FldA are shown. The spectra were recorded for 50-μM protein in an anaerobic buffer (50-mM potassium phosphate buffer, pH 7.0, and path length = 1 cm). The semireduced state was produced by stoichiometric addition of sodium dithionite. Excess dithionite was added to obtain the fully-reduced state. (b) Optically monitored potentiometric titration of FldA at 610 nm. The data (blue circles) and fit (dashed line) to the equation describing sequential one electron additions to a center with E_2 = −170 mV and E_1 = −190 mV. Sample contained 50 μM protein in an anaerobic buffer (10-mM potassium phosphate buffer, pH 7.0.) Path length = 1 cm. (c) Cyclic voltammetry of CjFldA (continuous blue line) adsorbed on a DDAB-coated pyrolytic graphite edge electrode. Cyclic voltammetry of the DDAB-coated electrode alone is also shown (broken gray line). Measurements performed in 50 mM potassium phosphate, pH 7 at 20°C with a scan rate of 20 mV/s. (d) Reduction of CjFldA by electrons from pyruvate via POR (red trace) or 2-oxoglutarate via OOR (Blue trace) in cell-free extracts monitored at 460 nm, as described in Section 4. The traces are an average of two determinations (raw data in the Supporting Information)

sample to FMN either within FldA or that had dissociated from the protein. Direct electrochemistry of bacterial flavodoxins using solid electrodes has been reported by several groups (Barker et al., 1988; Heering & Hagen, 1996; Seagel et al., 2017). From those findings, there are two points of particular significance for interpretation of the voltammetry of CjFldA. Firstly, peaks for the SQ/HQ transfor-mation are well-defined, whereas those of the Q/SQ transformation are typically absent. Secondly, free FMN typically contributes peaks with a mid-point potential of approximately −200 mV at pH 7. The voltammetry of CjFldA is consistent with Q/SQ *and* SQ/HQ mid-point potentials above −300 mV versus SHE. This conclusion is in agreement with the results from potentiometric titration. Based on voltammetry of CjFldA measured at several independently prepared electrodes and inspection of the relative peak heights and widths for the two processes, it is likely that the higher potential peaks de-scribe the contribution of free FMN. However, we cannot rule out

a contribution from the Q/SQ process at these potentials as noted in the voltammetry of *Azotobacter vinelandii* flavodoxin II studied at similarly DDAB-coated graphite electrodes (Seagel et al., 2017).

The E_1 and E_2 redox potential values determined from optical potentiometry (Figure 1b) are remarkably similar, and the E_1 value is far more electropositive than many flavodoxins (Table 1), despite the FMN isoalloxazine binding regions of CjFldA (the W-loop and Y-loop regions; Sancho, 2006) containing several D and E residues that might be expected to destabilize the anionic hydroquinone and shift the E_1 potential to more negative values (Table 1). This is further considered in Section 3.

The ability of FldA to act as electron acceptor for the POR and OOR enzymes was tested by adding cell-free extract plus CoA to the protein under anaerobic conditions and initiating the reaction by addition of either pyruvate or 2-oxoglutarate. A rapid reduction in the FMN absorbance in the 460-nm region was observed with either

TABLE 1 Comparison of redox potentials and FMN binding loop regions in selected flavodoxins and NrdI proteins

Species	Protein	pI	E1 (mV)	E2 (mV)	Δ (mV)	50s (W) loop	90s (Y) loop	Ref
D. vulgaris	Fld	4.0	−440	−143	297	STWGDDSIE	DSS--YE	Corrado et al. (1996)
Synechocystis	Fld	3.5	−433	−238	195	PTWWVGELQ	DQVGYAD	Bottin and Langoutte (1992)
A. vinlandii	Fld	4.4	−483	−187	296	PTLGEGELP	DQVGYPE	Seagel et al. (2017)
C. jejuni	Fld	3.9	−190	−170	20	STWGSGDLQ	DSESYSD	This study
						40s loop	**70s loop**	
E. coli	NrdI	9.4	−255	−264	−9	GGGGTAG	NRNFGEA	Cotruvo and Stubbe (2008)
B. cereus	NrdI	5.0	−309	−252	57	GFGNVPER	NRNWGDM	Gudim et al. (2018)
B. anthracis	NrdI	5.4	−385	−270	115	GFGNVPER	NRNWGDM	Berggren et al. (2014)

Note: The FMN is sandwiched between two loop regions known as the 50s or W-loop and 90s or Y-loop in classical flavodoxins, or the 40s loop and 70s loop in NrdI proteins. These contain aromatic/hydrophobic residues (highlighted in orange) that stack over the isoalloxazine ring. A preponderance of anionic residues (blue) in the loops in flavodoxins is thought to contribute to lowering of the E_1 redox potential in particular, whereas in NrdI proteins in the environment is more neutral or charge compensated (cationic residues in red).

substrate (Figure 1d). Although FldA has previously been identified as the electron acceptor for OOR (Weerakoon & Olson, 2008), these results show that POR also reduces FldA.

2.2 | Cj0559 (FqrB) is an NADPH: flavodoxin reductase related to those in Gram-positive bacteria

Cj0559 in *C. jejuni* is 46.3% identical with FqrB (HP1164) in *H. pylori* strain 26695, and these proteins are members of the large family of FAD containing pyridine nucleotide disulfide oxidoreductases (PNDORs), which include glutathione, CoA disulfide and mercuric reductases, although they do not contain a catalytic disulfide found in some other members of the family such as the thioredoxin reductases. The study of St Maurice et al., (2007) highlighted the conservation of FqrB-like proteins in the Campylobacterota, but similarities with PNDOR enzymes outside this group are less clear. Figure 2a shows a phylogenetic analysis of *C. jejuni* Cj0559 and a range of PNDOR homologs identified by BLAST analysis. It is apparent that the Campylobacterota enzymes, including Cj0559, cluster with a specific group of reductases from Gram-positive bacteria found in *Bacillus subtilis* (YpdA) and *Bacillus cereus/Banthracis anthracis* (FNR3) but are distinct from thioredoxin reductases and CoA disulfide reductases. YpdA is a putative bacillithiol disulphide reductase (Gaballa et al., 2010; Mikheyeva et al., 2019), and FNR3 enzymes have been characterized as flavodoxin reductases; *B. cereus* FNR3 can reduce NrdI, a specific flavodoxin required for formation of the tyrosyl radical in the Mn-containing class Ib RNR's in many Gram-positive bacteria (Lofstad et al., 2016). The FNR1 and FNR2 enzymes also reduce NrdI, with FNR2 being most efficient (Lofstad et al., 2016), but these are more distantly related to FqrB (Figure 2a).

We tested the ability of the purified C-terminally his-tagged recombinant Cj0559 to act as an NAD(P)H-dependent reductase for the flavodoxin FldA. *C. jejuni* Cj0559 was heterologously overproduced

and purified (Figure S1b) as a yellow-colored protein with an absorption spectrum typical of a flavoprotein with maxima at ~375 and ~460 nm (Figure 2b). In aerobic buffer at pH 7.5, it exhibited a low rate of NADPH oxidase activity (0.79 ± 0.07 μmol min^{-1} mg protein^{-1}, $n = 3$ determinations), but activity with NADH was over 10-fold lower (0.06 ± 0.01 μmol min^{-1} mg protein^{-1}, $n = 3$). When incubated under strictly anaerobic conditions with a molar excess of FldA, FqrB readily catalyzed the reduction of FldA with NADPH (Figure 2c and inset) but not with NADH (Figure 2d and inset). Using an estimated extinction coefficient for flavodoxin FMN of 12 mM^{-1} cm^{-1} at 460 nm (Mayhew & Tollin, 1992), we determined a rate of 14.5 ± 0.2 μmol FMN reduced min^{-1} mg FqrB protein^{-1} with NADPH as reductant ($n = 3$). These data show that *C. jejuni* FqrB is an efficient FldA reductase specific for NADPH.

2.3 | The growth defect of an *fqrB* mutant is partially responsive to dRNS

Given the phylogenetic relationship noted above between FqrB and some NrdI reducing PNDOR enzymes in Gram-positive bacteria, and the identification of FqrB as a redox partner for FldA, we sought in vivo evidence that FqrB might be involved in ribonucleotide reduction. Although *hp1164* (*fqrB*) was reported to be essential in *H. pylori*, we were able to construct a deletion mutant in the *cj0559* gene by replacing most of the coding region with a nonpolar kanamycin-resistance cassette via allelic exchange mutagenesis (see Section 4). The mutant was also complemented with a wild-type gene copy inserted at the *cj0046* pseudogene locus, driven by the *metK* promoter. The mutant formed small colonies on plates, and in liquid culture on complex media, it exhibited a significant growth defect compared with the wild-type and complemented strain (Figure 3a). When grown with a mixture of all four deoxyribonucleosides (dRNS) at 0.1 mM each (final concentration), the growth
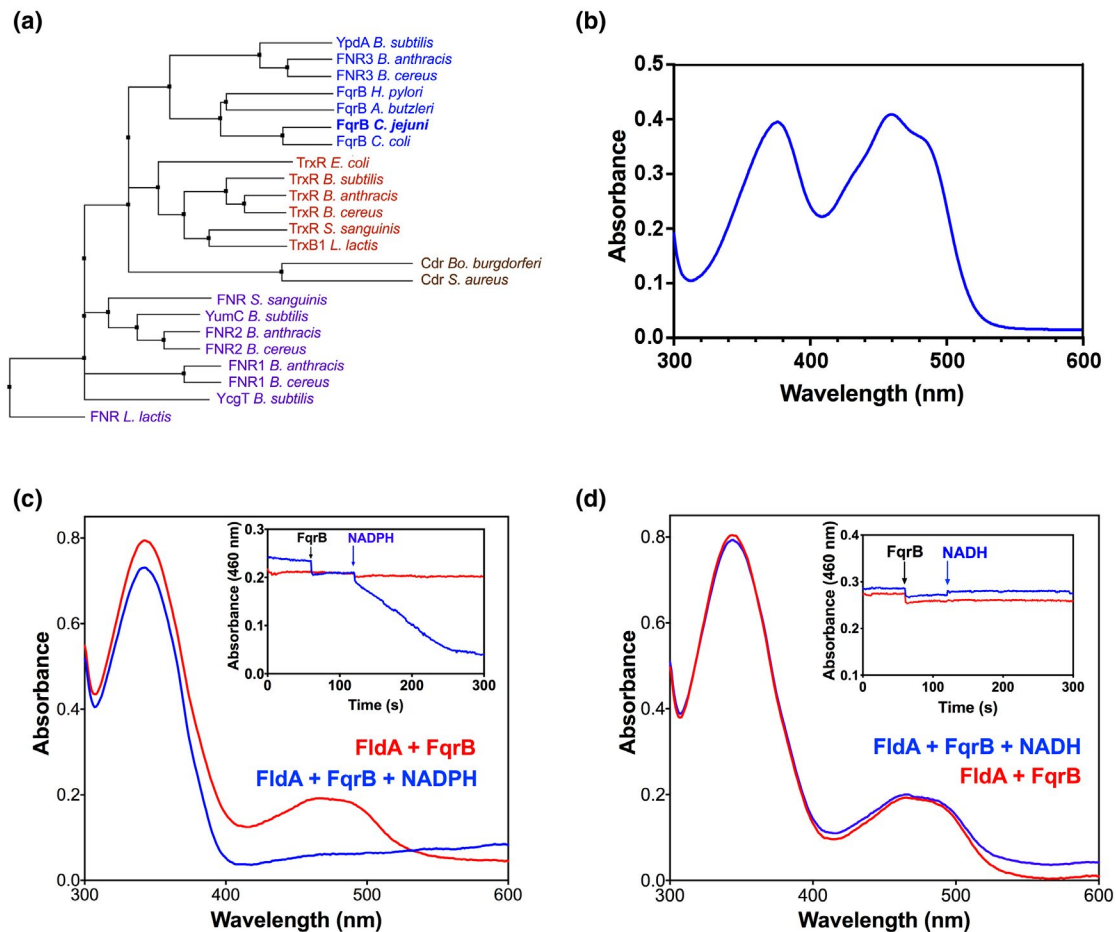
FIGURE 2 FqrB is related to flavodoxin reductases in Gram-positive bacteria and is an NADPH specific FldA reductase. (a) Phylogenetic tree of a selection of PNDOR enzymes from Gram-negative and Gram-positive bacteria. A multiple sequence alignment was generated in CLUSTAL omega then JALVIEW used to construct the tree shown. Sequences were obtained from UNIPROT. Genus abbreviations; *A.*, *Arcobacter*; *B.*, *Bacillus*; *Bo.*, *Borrelia*; *C. Campylobacter*; *E.*, *Escherichia*; *H.*, *Helicobacter*; *L.*, *Lactobacillus*; *S.*, *Staphylococcus*; *St.*, *Streptococcus*. (b) UV-VIS absorption spectrum of purifed *C. jejuni* FqrB (50 µM) with FAD peaks at 375 and 460 nm. (c) NADPH dependent reduction of FldA catalyzed by FqrB. The absorbance spectrum of a mixture of FldA (50 µM) and FqrB (0.1 µM) in 50-mM Tris-HCl buffer pH 7.5 was recorded alone (red trace) or 5 min after the addition of NADPH (0.15-mM final concentration). The *inset* shows a kinetic trace at 460 nm, to show the FldA FMN reduction. (d) The same as (c) but with NADH

of the wild-type and complemented strain were not significantly different from that of the controls, whereas the mutant showed an increased growth rate. Interestingly, in the presence of a higher concentration (1 mM each) of dRNS, the growth rate and final cell density of the wild-type and complemented strain were severely inhibited, an effect probably due to an imbalance in the intracellular concentrations of DNA precursors (Torrents, 2014). However, the growth of the *fqrB* mutant was much less affected (Figure 3a). The mutant was also significantly less sensitive to the toxic nucleotide analogs 6-thioguanine and 6-mercaptopurine compared with the wild-type and complemented strains (Figure 3b). Taken together, these results suggest that the lack of FqrB in the mutant affects dRNS uptake and metabolism; a slower conversion of ribonucleotides to deoxyribonucleotides via ribonucleotide reductase might explain the partial growth stimulation by exogenous dRNS. We further investigated the link between FqrB and RNR by in vitro studies with the beta subunit of the RNR.

2.4 | Characterization of NrdB, the RNR beta subunit of *C. jejuni*

Campylobacter jejuni NCTC 11168 encodes a single heterodimeric RNR (Parkhill et al., 2000). The alpha subunit (NrdA; Cj0024) is predicted to catalyse ribonucleotide reduction using a cysteine radical, generated by long-range transfer from a tyrosine radical formed in the beta subunit (Cj0231). In class Ia RNRs, the tyrosine radical in NrdB is generated by oxygen and electrons from two reduced iron centers in a µ-oxo-bridged configuration, whereas in class Ib enzymes that have oxygen unreactive manganese ions instead of iron, superoxide generated by a reduced flavodoxin (NrdI) is used to form the radical in the beta subunit, designated NrdF (Stubbe & Cotruvo, 2011). As noted above, NrdI is itself reduced by a specific reductase of the PNDOR family. The dRNS growth stimulation observed in the *C. jejuni fqrB* mutant (Figure 3a) could be explained if radical formation in the *C. jejuni* RNR required FldA, with FqrB acting
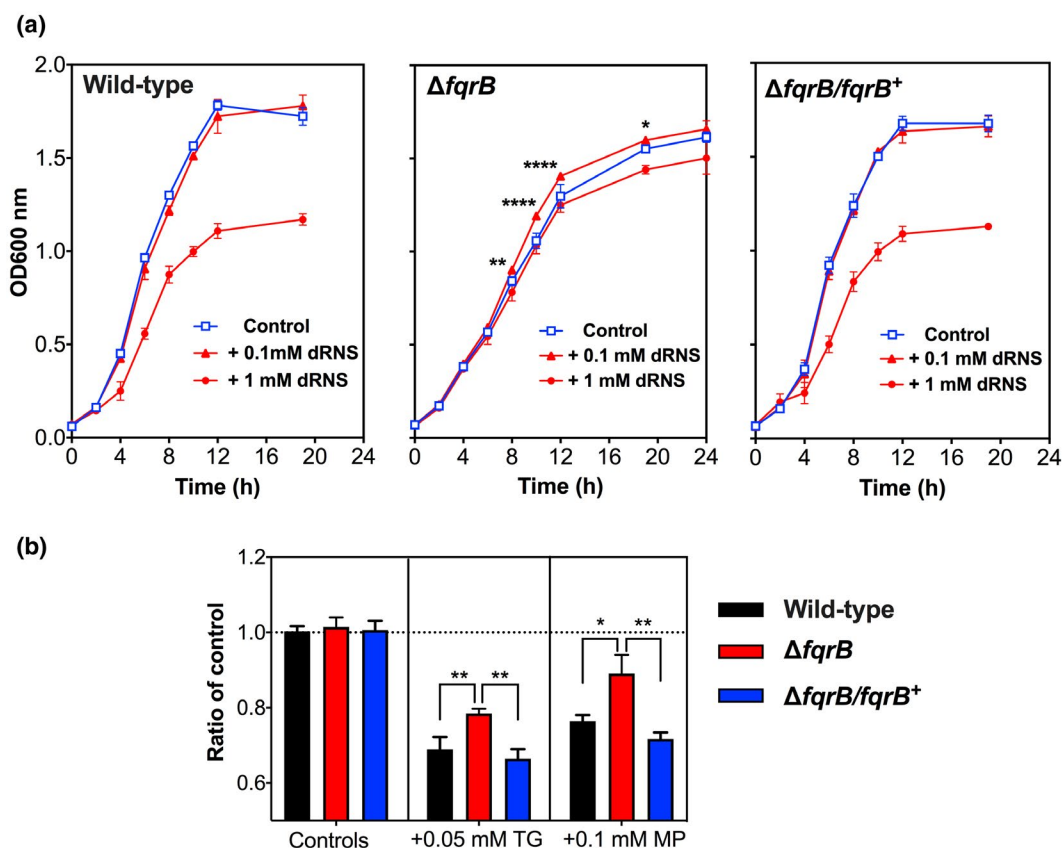
FIGURE 3 Growth phenotypes of wild-type, *fqrB* mutant and complemented strains and effect of deoxyribonucleosides or toxic analogs. (a) Growth curves of wild-type (left panel), *fqrB* mutant (middle panel), and complemented strain (right panel) under standard microaerobic conditions in complex MHS media are shown in the absence or the presence of the indicated concentrations of a mixture of the 4 deoxyribonucleosides (dRNS). The data points are means of triplicate independent cultures with error bars indicating *SD*. For the *fqrB* mutant, Student's *t*-test was used to examine the signficance of the effect of 0.1-mM dRNS compared with control (****$p < .0001$; **$p < .01$; *$p < .05$). (b) The effect of the toxic nucleotide analogs 6-thioguanine (TG) and 6-mercaptopurine (MP) on wild-type (black bars), *fqrB* mutant (red bars), and complemented strain (blue bars) were evaluated by growth in MHS media. Cultures as in (a) were set up in triplicate and the OD600 nm measured after 12 hr. The data are expressed as a ratio of the controls without TG or MP addition. Error bars show *SD* and the significance of the effect of TG or MP estimated by Student's *t*-test (**$p < .01$; *$p < .05$)

as a physiologically relevant flavodoxin reductase. However, CjFldA is distinct from NrdI proteins and the alpha and beta subunits of *C. jejuni* RNR and other Campylobacterota are related to other class Ia NrdA and NrdB proteins from Gram-negative bacteria (although it should be noted that Cj0231 is currently annotated as NrdF). The *C. jejuni* NrdA subunit also has a typical N-terminal ATP-cone domain that is characteristic of a class Ia enzyme (Hofer et al., 2012). Therefore, we wished to test if radical formation in *C. jejuni* NrdB required flavodoxin, by producing purified radical free NrdB and reconstituting with FldA, FqrB, and NADPH to determine if the radical could be regenerated in vitro.

NrdB was overproduced in *E. coli* BL21 (DE3) as a C-terminally his-tagged protein and purified by nickel affinity chromatography. Two bands were consistently seen on SDS-PAGE gels (Figure S1c), an upper band corresponding to the expected size of NrdB-6His (~40.5 kDa) and a lower band of ~35 kDa. Both bands were trypsin digested and subjected to HPLC-LC/MS. The same NrdB peptides were detected in both bands (Figure S2 and Table S2), including from both the N-terminal and C-terminal regions of NrdB, showing

that the lower band is not a contaminant or N-terminally truncated version of the upper band. It most likely arises due to an unidentified post-translational modification, which causes faster mobility on SDS-PAGE. The metal content of independently purified batches of the protein was determined by inductively coupled plasma mass spectrometry (ICP-MS) after growth in either unsupplemented, iron- or manganese-supplemented media (Figure 4a). In each case, the molar ratio of Fe/protein (1.0, 1.4, and 0.85, respectively) was significantly higher than the Mn/protein ratio (0.14, 0.05, and 0.25, respectively). Overall, the data confirm that the *C. jejuni* RNR is indeed an Fe enzyme of the class Ia type and that the database annotation of Cj0231 as NrdF is incorrect. Although the expected ratio of Fe/monomer is 2, a suboptimal stoichiometry is commonly found in heterologously expressed RNRs (Roca et al., 2008). The optical absorption spectrum of the protein shows a typical sharp feature at 410–411 nm diagnostic of the presence of a stable tyrosyl radical as well as weaker charge transfer bands centered around 325 and 370 nm arising from the μ-oxo-bridged diferric center. We found that treatment of the protein with 1 mM of the radical scavenger
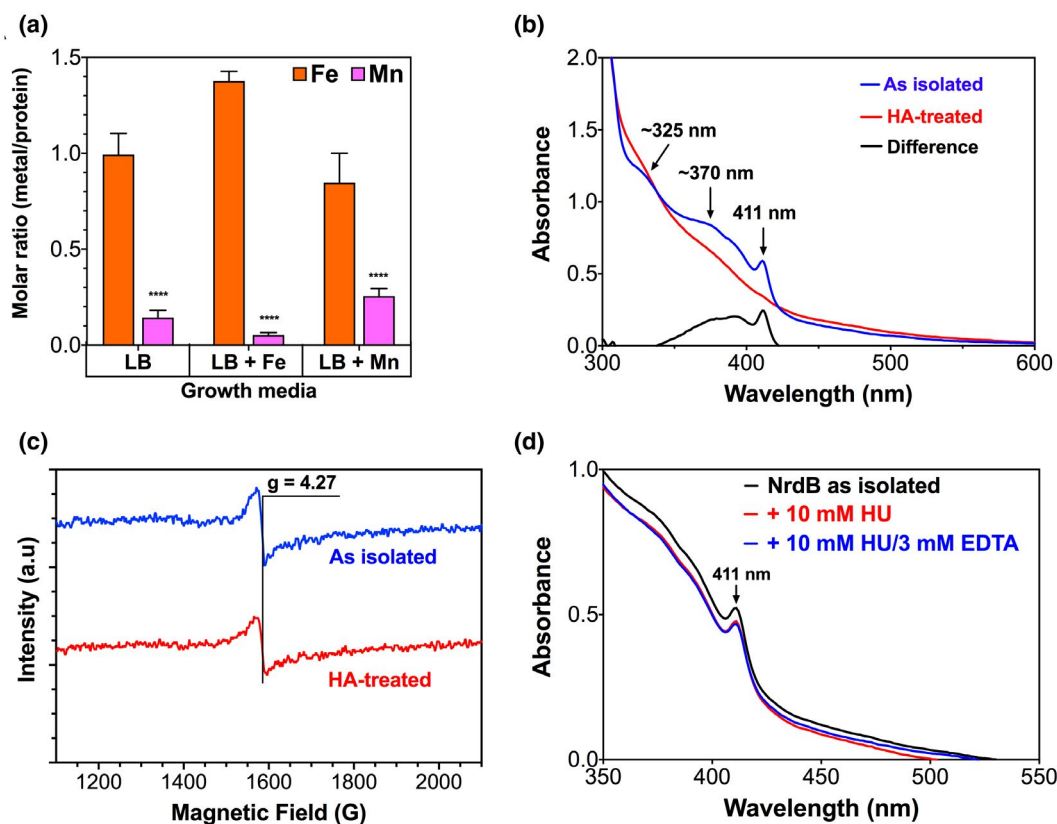
FIGURE 4 Characterization of the NrdB subunit of *C. jejuni* RNR. His-tagged NrdB was purified from *E. coli* BL21 (pETNrdB) as described in Section 4. (a) Iron (orange) and manganese (pink) content of NrdB, measured by ICP-MS. The data are the means and *SD* of three independent purifications from cells grown in LB alone, LB + Fe (50-µM ferrous ammonium sulfate) or LB + Mn (50-µM manganese chloride). The sulfur content of the samples was used to normalize the data to the protein content (Wang et al., 2010) and is expressed as a molar ratio. In each case, the Mn ratio is significantly lower than the Fe ratio (****$p < .0001$ by Student's *t*-test). (b) Optical absorption spectroscopy of NrdB. The blue trace shows the spectrum of as-purifed NrdB (100 µM) with the tyrosyl radical peak at 411 nm and charge transfer bands of the di-ferric center at 325 and 370 nm. The red trace shows the spectrum after 30-min treatment with 1-mM hydroxylamine (HA), which quenches the radical. The black trace is the difference spectrum, illustrating the tyrosyl radical contribution. The EPR spectrum in (c) shows that HA treatment does not significantly alter the $g = 4.27$ CW EPR signal of the high spin ferric iron in rhombic coordination in 50-µM NrdB as isolated (blue trace) or 50-µM NrdB + 1-mM hydroxylamine (red trace). Instrumental conditions used were: microwave frequency $\nu_{MW} = 9.47$ GHz; microwave power $P_{MW} = 3.165$ mW; sweep rate $v = 22.65$ G s^{-1} (one scan); time constant $\tau = 81.92$ ms; modulation amplitude $A_m = 5$ G; modulation frequency $\nu_m = 100$ kHz; registration temperature $T = 10$ K. In (d), optical spectroscopy (50-µM NrdB) shows that a high concentration of hydroxyurea (HU), either with (blue trace) or without (red trace) EDTA does not appreciably quench the tyrosyl radical compared with HA in panel (b)

hydroxylamine (HA) for 30 min efficiently removed the tyrosyl radical, as evidenced by the disappearance of the 411-nm band (Figure 4b). Although the optical spectrum of the HA treated protein also appeared to lack the 370 nm absorbance associated with the di-ferric center, comparison of the electron paramagnetic resonance (EPR) spectra of the as-purifed and HA-treated protein showed an equivalent feature at $g = 4.27$ attributable to residual magnetically isolated ferric iron (Figure 4c). Calculation of the difference spectrum of HA treated versus untreated protein (Figure 4b) and applying a literature value for the extinction coefficient of 3.25 mM cm^{-1} for the radical (Petersson et al., 1980) resulted in an estimation of the radical yield in the purified protein of 0.7 per monomer, comparable with data for other enzymes (Roca et al., 2008). In contrast to HA, treatment with the commonly used radical scavenger hydroxyurea

(HU) did not result in quenching, even in the presence of the metal chelator EDTA (Figure 4d).

2.5 | Tyrosyl radical regeneration in NrdB can be catalyzed by FldA, FqrB, and NADPH

The ability to produce a radical free NrdB preparation allowed us to investigate the requirements for radical formation in this protein. Incubation of HA-treated and dialyzed NrdB with an equimolar concentration of the flavodoxin FldA (50 µM) plus a catalytic amount of FqrB (5 µM) and excess NADPH resulted in the build up of the characteristic tyrosyl radical absorbance at 411 nm (Figure 5a). A series of control incubations lacking any single component of this mixture
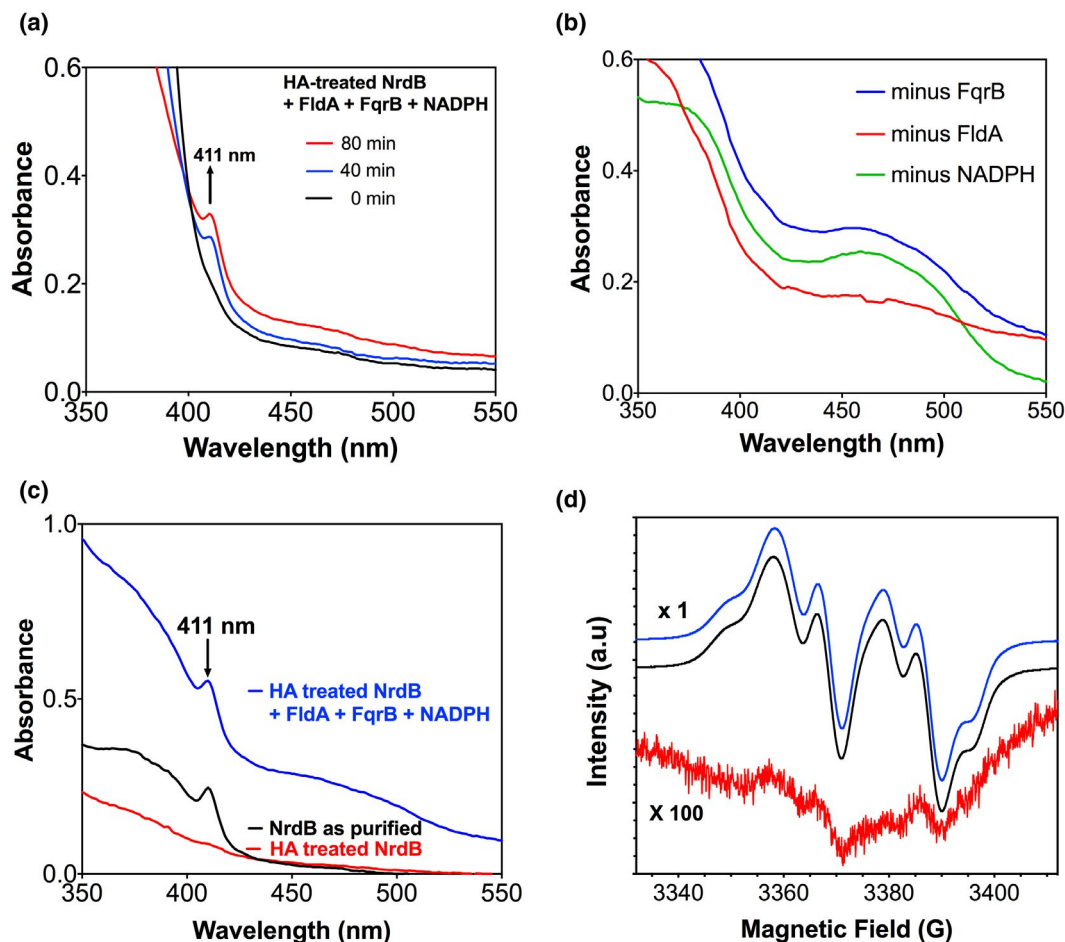
FIGURE 5 Reduced flavodoxin catalyzes tyrosyl radical regeneration in NrdB. In panel (a), a mixture of hydroxylamine-treated NrdB (50-μM final concentration), FldA (50 μM), FqrB (5 μM), and NADPH (1 mM) in 50-mM Tris-HCl buffer pH 7.5 was incubated at 37°C and spectra recorded at the times shown. The build-up of the tyrosyl radical in NrdB is evident at 411 nm. In (b), the spectra of a series of control incubations missing one of the components in (a), as indicated, was obtained after 80-min incubation at 37°C. In (c), the same mixture as in panel (a) was prepared, incubated for 80 min and the optical spectra compared with as-purifed NrdB and HA-treated NrdB. These same samples were then examined by EPR spectroscopy (d) as described in Section 4. The free radical area of the CW EPR spectra of NrdB is shown: 50-μM NrdB as isolated shows a typical EPR line shape of a RNR tyrosyl radical (black trace); 50-μM NrdB +1-mM hydroxylamine results in essentially complete reduction of the radicals (red trace); the free radical reconstituted by 50-μM flavodoxin (FldA) and 5-μM flavodoxin reductase (FqrB) in the presence of 1-mM NADPH (blue trace) has a line shape indistinguishable from that of NrdB as isolated. The instrumental conditions were microwave frequency $\nu_{MW} = 9.47091$ GHz (blue trace), 9.46769 GHz (black trace) and 9.47058 GHz (red trace; the three spectra were shifted along the magnetic field axis to a common g-value on the basis of these differences in the microwave frequencies); $P_{MW} = 5.016 \times 10^{-2}$ mW; $v = 0.596$ G s^{-1} (one scan); $\tau = 81.92$ ms; $A_m = 3$ G; $\nu_m = 100$ kHz; $T = 10$ K. Symbol "x" gives relative magnification of the spectra

resulted in no increase in absorbance at 411 nm (Figure 5b), showing that radical formation was dependent on reduced flavodoxin formed through the NADPH dependent reductase activity of FqrB. In order to further confirm that the tyrosyl radical had indeed been regenerated in the reconstituted system with characteristics similar to the native NrdB, we compared the EPR spectrum of a sample of as-purified NrdB with HA-treated NrdB and that obtained after reconstitution with NADPH, FqrB, and FldA. The optical spectra of the same samples used for EPR are shown in Figure 5c, which again confirm the presence of the 411 nm band after reconstitution, and the corresponding 10 K EPR spectra are shown in Figure 5d. Essentially, identical EPR spectra were recorded from both the as-purified protein and after reconstitution with NADPH, FqrB, and FldA

(Figure 5d). The spectra also show that HA treatment effectively removed the radical from NrdB, with only very weak EPR signals remaining. The center of the free radical EPR signals is at ~$g = 2.0052$, and the lineshape is typical of that of Fe$_2$-tyrosyl radical containing class Ia RNRs (Hoganson & Babcock, 1992; Sahlin et al., 1987).

2.6 | Is superoxide involved in FldA catalyzed tyrosyl radical formation?

The di-ferrous center in class Ia RNRs is readily oxygen reactive, and the electron input required for re-reduction has been proposed to be supplied in some bacteria by a small ferredoxin, YfaE (Wu

et al., 2007). *yfaE* is sometimes genetically linked to the *nrdAB* genes but is not present in Campylobacterota including *C. jejuni*. Given the *C. jejuni* RNR is a class Ia enzyme, it seems most likely that the role of FldA identified above is as a simple electron donor to NrdB in place of YfaE. However, in class 1b RNRs that use oxygen unreactive Mn as cofactor, the NrdI flavodoxin generates superoxide that acts as the oxidant to form the tyrosyl radical (Berggren et al., 2014). The possible involvement of superoxide in the regeneration of the tyrosyl radical in the *C. jejuni* NrdB by reduced FldA was investigated in two ways. First, we added excess superoxide dismutase to a mixture of FqrB, FldA, and HA-treated NrdB before adding NADPH to start the reaction. After prolonged incubation, tyrosyl radical formation was only slightly suppressed compared with incubations lacking SOD (Figure 6a,b), but was still readily detectable. The caveat here is that superoxide could be channeled from flavodoxin to NrdB by close interaction, so may not be sensitive to SOD (Berggren et al., 2014). Secondly, we incubated purifed HA-treated NrdB with the well-known xanthine oxidase/hypoxanthine superoxide generating system, as a way of generating superoxide independently of flavodoxin and FqrB. A time-dependent formation of the tyrosyl radical could be observed, as evidenced by the absorbance increase at 411 nm (Figure 6c). This suggests that at least in vitro superoxide can result in tyrosyl radical formation in *C. jejuni* NrdB.

3 | DISCUSSION

As the electron acceptor for the citric-acid cycle enzymes POR and OOR, FldA is a central redox shuttle in the physiology of *C. jejuni*, but other roles for this key protein have not been investigated, and

genetic studies are hampered by its essentiality. In this work, we have identified the *cj0559* encoded FqrB as an FldA reductase and phenotypic analysis of a deletion mutant lacking FqrB has revealed a hitherto unknown link between FldA and deoxyribonucleotide reduction.

FqrB from *C. jejuni* is an NADPH-specific flavodoxin reductase that has a phylogenetic relationship to a group of similar enzymes from Gram-positive bacteria, some of which are known to be redox partners for NrdI-like flavodoxins necessary for tyrosyl radical formation in class Ib RNRs. FqrB was initially identified in *H. pylori* as a quinone and flavodoxin reductase that was suggested to participate in the production of NADPH by operating in the reverse direction to that proposed here, that is, coupling the reduction of NADP to the oxidation of reduced flavodoxin that had been generated by the action of POR (St Maurice et al., 2007). This seemed to confirm earlier data from the study of Hughes et al., (1998) who detected pyruvate-, CoA-, and FldA-dependent NADPH production in *H. pylori* cell-free extracts (CFE). The same reaction could also be demonstrated in *C. jejuni* crude extracts (St Maurice et al., 2007). However, the rates of NADPH production in these studies were very low (of the order of a few nmol/min mg protein^{-1}). We can now explain this in view of the relatively high midpoint redox potential of FldA (−180 mV) compared with NADPH (−320 mV), such that it is thermodynamically unfavorable for FldA to reduce NADP. It is therefore unlikely that this mechanism would be relevant in vivo, and it should be noted that other known enzymes in *C. jejuni* central metabolism operate to reduce NADP directly (e.g., isocitrate dehydrogenase). On the contrary, our data suggest that FqrB catalyzes NADPH-dependent reduction of FldA, in addition to POR and OOR, and this contributes to the maintenance of a reduced pool of FldA for diverse metabolic reactions
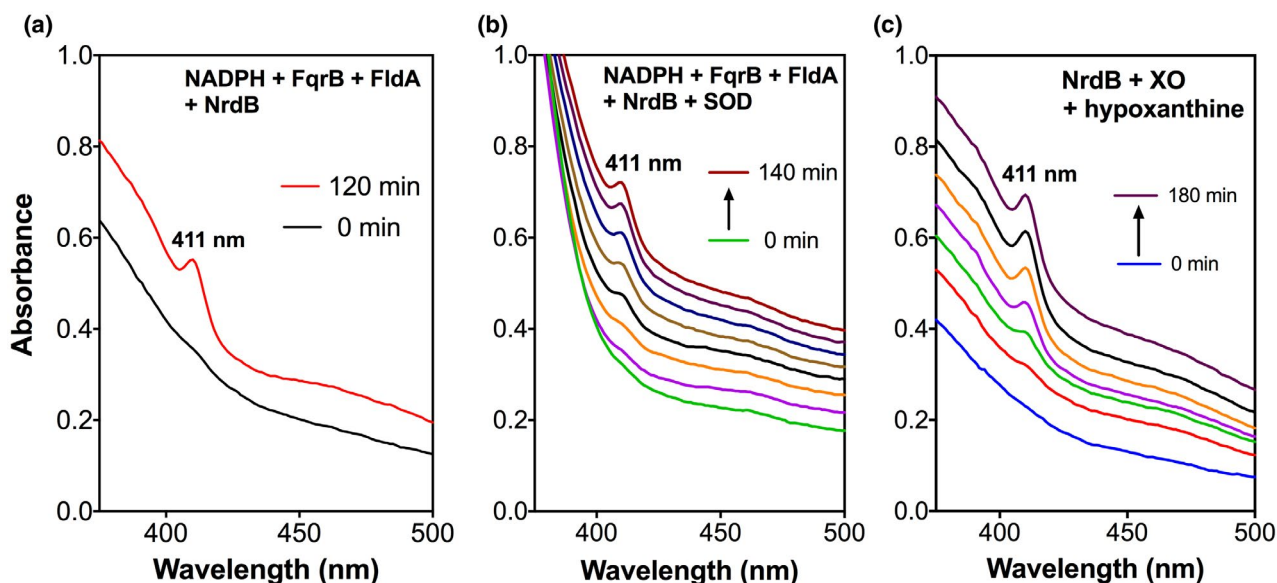
FIGURE 6 Superoxide can catalyze tyrosyl radical formation in NrdB in vitro. In panel (a), the complete reconstituted system of HA-treated NrdB (50 μM), FldA (50 μM), FqrB (5 μM), and NADPH (1 mM) was incubated at 37°C for 120 min as a control to show formation of the tyrosyl radical at 411 nm. In panel (b), the same components were incubated but with the addition of 20 units of SOD and the spectra recorded at 20-min intervals for the times shown. In panel (c), HA-treated NrdB alone (50 μM) was incubated at 37°C with 1 mM hypoxanthine and 0.5 units of xanthine oxidase for 3 hr and spectra recorded every 30 min as shown
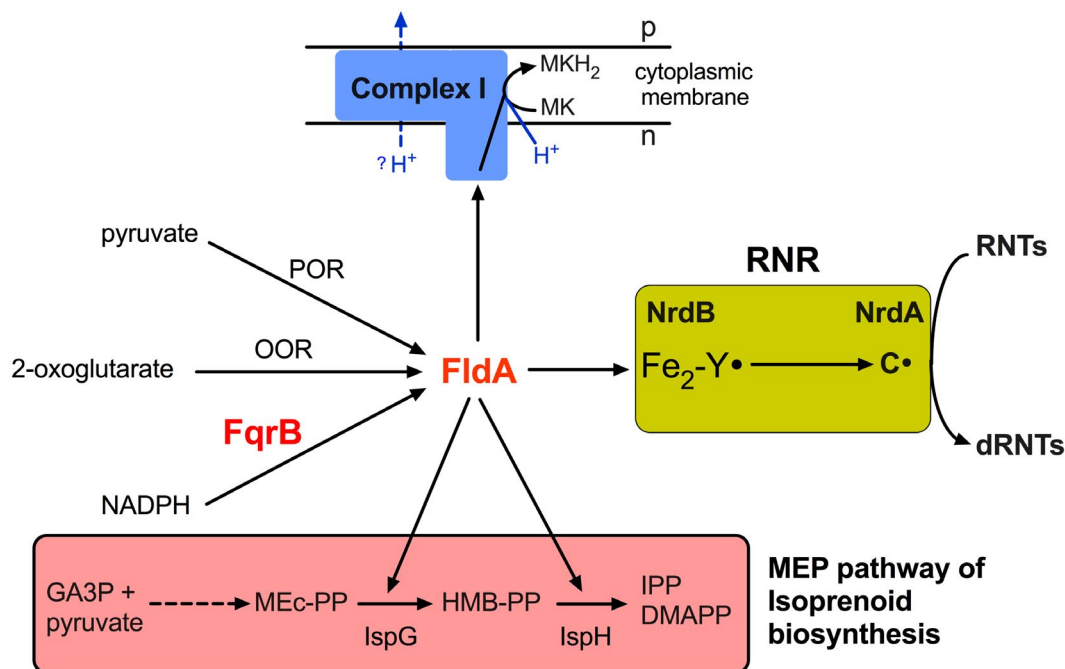
FIGURE 7 Multiple pathways for FldA reduction and the role of FldA in electron transport, isoprenoid biosynthesis, and deoxyribonucleotide reduction. FldA can be reduced by electrons from at least three sources; from pyruvate oxidation via pyruvate:flavodoxin oxidoreductase (POR), from 2-oxoglutarate reduction via 2-oxoglutarate:flavodoxin oxidoreductase (OOR) or from NADPH oxidation via flavodoxin quinone reductase (FqrB). FldA is the only known electron donor for respiratory Complex I in *C. jejuni*, but given the relatively small redox potential difference (~100 mV) between $FldA_{ox}$/$FldA_{red}$ couple and the menaquinone (MK)/menaquinol (MKH_2) couple, it is unclear if Complex I is proton translocating. Our results suggest that FldA is an electron donor to the NrdB subunit of ribonucleotide reductase (RNR), to generate the tyrosine radical (Y•). This is then transferred to the NrdA subunit to generate a radical at the active site cysteine (C•), necessary for reduction of ribonucleotides (RNTs) to deoxyribonucleotides (dRNTs). FldA is also thought to be required as a source of electrons for two consecutive steps in the final section of the MEP isoprenoid biosynthesis pathway, catalyzed by IspG which converts methylerythritol cyclic pyrophosphate (MEc-PP) into 4-hydroxy-3-methylbut-2-enyl pyrophosphate (HMB-PP) and IspH which converts HMB-PP into the products isopentyl pyrophosphate (IPP) and dimethylallyl pyrophosphate (DMAPP). MEc-PP is produced in several enzymatic steps from pyruvate and glyceraldehyde-3-phosphate (GA3P)

requiring this electron carrier (Figure 7). That NADPH can reduce FldA might also explain previous reports of (albeit low) NADPH dependent respiration in membranes and cell extracts of campylobacters (Lascelles & Calder, 1985; Weerakoon & Olson, 2008).

The phenotype of an *fqrB* deletion mutant implicates FqrB in ribonucleotide reduction. The fact that this mutant was viable, although with a growth defect, is presumably because POR and OOR are also still able to contribute to FldA reduction. Although POR is essential (Kendall et al., 2014), presumably because there is no other way to make acetyl-CoA, an *oorB* mutant has previously been reported (Weerakoon & Olson, 2008). The stimulation of *fqrB* mutant growth by dRNS was significant although not large in magnitude, but this would be consistent with the additional functions that FldA has in electron transport to Complex I and, for example, isoprenoid biosynthesis (Figure 7) as well as other possible cellular redox processes yet to be identified. It should also be noted that although a potential transport system and phosphoribosyl phosphotransferase for nucleotide salvage has been identified in *C. jejuni* (Yahara et al., 2017), Campylobacterota including *C. jejuni* are not thought to possess a deoxyribonucleoside kinase that would efficiently phosphorylate dRNS (Konrad et al., 2012; Sandrini et al., 2006), which could

account for the poor growth response observed. It is also possible that FqrB can reduce other, as yet unidentified, redox partners that are important for optimum growth.

Biochemical evidence for a role of FqrB and FldA in RNR activation was obtained by an in vitro reconstitution approach with the relevant purified proteins. The tyrosyl radical in purified NrdB was remarkably resistant to quenching by HU, despite growth being sensitive to this compound and causing filamentation in treated cells consistent with RNR inhibition (Sellars et al., 2002). HA proved an effective radical scavenger however and we were able to show, with appropriate controls, that radical reformation could be promoted in the presence of NADPH, FqrB, and FldA. Importantly, the EPR data show that the characteristics and environment of the radical formed in vitro is indistinguishable from that in the as-purifed NrdB protein. The *fqrB* mutant phenotype data taken together with the in vitro reconsitution experiments therefore support a physiological role for FqrB and FldA in NrdB tyrosyl radical formation, and thus ribonucleotide reduction, in *C. jejuni*, as illustrated in Figure 7. Although our data were obtained with strain NCTC 11168, FqrB, FldA, and NrdB are present in other strains of *C. jejuni* and, for example, are 97%–100% identical in two other commonly studied strains, 81–176

and 81116. The model in Figure 7 should therefore be generally applicable.

We have characterized FldA in this work as a high redox potential flavodoxin, with the $FldA_{ox}/FldA_{sq}$ and $FldA_{sq}/Fld_{hq}$ couples having E_m values of −170 and −190 mV, respectively. Before we consider the significance of this in relation to RNR, it is worth noting the implications of these redox properties for understanding the bioenergetics of Complex I in *C. jejuni*, which uses FldA as the electron donor instead of NADH. Aerobic bacteria that use NADH (E_m − 320 mV) coupled with ubiquinone (E_m + 100 mV) as the electron acceptor for Complex I will have an overall ΔE of ~ 420 mV to drive proton translocation electrogenically, against an existing Δp of ~ 180 mV. However, only menaquinone-8 (MK-8) and methylmenaquinone-8 (mMK-8) are present in *C. jejuni* membranes (Carlone & Anet, 1983). The E_m for MK-8 is about −75 mV, and for mMK-8, it is −124 mV (Juhnke et al., 2009) or as low as −140 mV (Hein et al., 2018). The ΔE for FldA reduction of MK-8 is therefore only ~100 mV, and for mMK-8, it is ~50 mV; considerably lower than Δp. Unless the in vivo redox potentials of the menaquinones and/or the FldA flavin are considerably different from those measured in solution, it remains an open question if electrogenic proton pumping can occur through Complex I in *C. jejuni* (see also Taylor & Kelly, 2019). Interestingly, direct measurements of Δp in intact *C. jejuni* cells using ion-selective electrodes showed that pyruvate produced the lowest Δp compared with electron donors like formate, that do not couple with FldA (van der Stel et al., 2017).

Canonical flavodoxins involved in electron transport usually have a wide separation in their E_1 and E_2 redox potentials, due to a negative electrostatic environment around the isoalloxazine ring of the FMN, causing destabilization of the hq form and shifting the E_1 potential much more negative than free FMN. For example, *Desulfovibrio vulgaris*, *Synechocystis*, and *A. vinelandii* all have E_1 values of <−400 mV (Table 1). This is also reflected in the pI values of such flavodoxins, which are usually acidic. NrdI proteins, however, have a bi-modal distribution with both low pI (mainly Firmicutes) and high pI (*E. coli* and most other proteobacteria) types (Johansson et al., 2010). Both types tend to have a more neutral (or charge compensated) environment in the loops surrounding the bound FMN, resulting in higher and often more similar E_1 and E_2 redox potentials than canonical flavodoxins (Table 1), but the picture is quite complex and other residues are also important.

The *C. jejuni* FldA is a long-chain flavodoxin with a predicted pI of 3.9, and it possesses conserved anionic residues in the W- and Y-loop regions involved in FMN binding (Table 1) that might be expected to result in a much lower E_1 redox potential than the −190 mV determined here. A crystal structure will be needed to rationalize the reasons for this disparity. Nevertheless, the similarity in the smaller separation in the E_1 and E_2 potentials of FldA and most NrdI proteins is intriguing. In class Ia RNRs, a small ferredoxin, exemplified by YfaE in *E. coli* (Wu et al., 2007) has been implicated in supplying electrons to reduce the di-ferric centre in NrdB to allow oxygen to react with the di-ferrous state, necessary to form the tyrosyl radical. No homologue of YfaE exists in *C. jejuni* and indeed only 29% of 181 NrdAB containing genomes were found to encode a *yfaE*-like gene linked to

nrdAB (Wu et al., 2007), implying that in most bacteria, other redox proteins satisfy this requirement. Our data suggest that *C. jejuni* uses the flavodoxin FldA instead of a ferredoxin as the electron donor to NrdB. YfaE is a 2Fe-2S ferredoxin that directly supplies electrons, one at a time, to reduce the NrdB diferric center (Wu et al., 2007). FldA, with E_1 and E_2 separated by only 20 mV could act in a similar manner. Nevertheless, in vitro generated superoxide also formed the radical in NrdB, as found with the NrdI flavodoxins interacting with the class Ib NrdF (Berggren et al., 2014). However, the physiological significance of this is difficult to judge, given that the NrdB/class Ia type of Fe-containing RNR should be fully capable of generating the Tyr radical from the oxidation of ferrous to ferric iron at the di-iron center mediated by molecular oxygen alone. It would clearly be informative to examine the relative reactivity of the *C. jejuni* NrdB di-iron center with superoxide versus oxygen in more detail.

In conclusion, our results explain why the sole flavodoxin of *C. jejuni* is essential and provide experimental evidence for at least one key role unrelated to respiratory electron transport. Recent work on the *H. pylori* FldA has resulted in the development of inhibitors that are novel drug candidates for therapeutic use (Salillas & Sancho, 2020), highlighting how the unique biochemistry of essential proteins like flavodoxin in pathogenic Campylobacterota can be exploited.

4 | EXPERIMENTAL PROCEDURES

4.1 | Bacterial strains and growth conditions

C. jejuni NCTC 11168 was routinely grown at 42°C in microaerobic conditions [10% (v/v) O_2, 5% (v/v) CO_2 and 85% (v/v) N_2] in a MACS growth cabinet (Don Whitley Scientific, Shipley, UK). Columbia blood agar plates containing 10 µg/ml each of amphotericin B and vancomycin were used for routine subculture. For *fqrB* mutant selection, kanamycin was additionally used in blood agar plates at 50 µg/ml, and for selection of the complemented mutant, both kanamycin and apramycin (50 µg/ml each) were included. Cells from plates were inoculated into 25-ml starter cultures in Mueller–Hinton broth supplemented with 20-mM L-serine and 10 µg/ml each of vancomycin and amphotericin B (MHS media). Starter cultures were incubated on a shaker at 150 rpm in the MACS growth cabinet for 12–16 hr followed by inoculation into growth cultures (30–500 ml) to a starting OD_{600} of ~0.1. *E. coli* strains were grown aerobically in LB media at 37°C. Where required ferrous ammonium sulfate or manganese chloride was added to 100 µM final concentration and carbenicillin used at 50 µg/ml.

4.2 | Construction of an *fqrB* mutant and complemented strain

Isothermal assembly (ISA) cloning (Gibson et al., 2009) was used to generate a plasmid for transformation into *C. jejuni*, that deletes

cj0559 (*fqrB*) by allelic exchange mutagenesis, replacing most of the coding region with a kanamycin resistance cassette derived from pJMK30 (van Vliet et al., 1998), which carries a constitutive promoter and no terminator. The ISA reaction assembled 4 PCR amplified fragments; HincII digested pGEM3Zf(-) vector, two regions of ~500 bp flanking *cj0559*, such that only the first few and last few codons of the gene were retained, and the kanamycin resistance cassette, to be inserted between the two flanking regions. The kanamycin resistance cassette was amplified from pJMK30 using primers Kan_F and Kan_R (Table 2). The left flanking region of the gene was amplified using primers FQRB_ISA_F1F and F1KR (Table 2), and the right flanking region was amplified by FQRB_ISA_F2KF and F2R. The F1F and F2R primers contain 30-bp adapters for the pGEM3Sf(-) vector cut with HincII and the F1KR and F2KF primers contain 30-bp adapters for the kanamycin resistance cassette. PCR amplifications were performed with phusion polymerase (NEB). The ISA reactions were performed as previously described (Liu & Kelly, 2015) and used to directly transform competent *E. coli* DH5α cells, with selection on LB + kanamycin agar plates. Colonies were screened by PCR with using different combinations of KAN, ISA, and standard M13 primers. Correct plasmids, designated pGEMFQR were confirmed by automated DNA sequencing (Core Genomic Facility, University of Sheffield Medical School, UK). pGEMFQR was electroporated into *C. jejuni* NCTC 11168 and cells plated out on Columbia agar plates, incubated overnight in microaerobic conditions at 42°C. The growth was then transferred to Columbia blood agar plates plus kanamycin and incubated for 3 days. Correct mutants were identified by colony PCR with ISA and KAN primers. To complement this mutant with the wild-type *fqrB* gene driven by its native promoter, the gene plus ~200 bp upstream sequence was amplified with primers FQRB_COMP_F and FQRB_COMP_R (Table 2) and cloned into the pRRA

vector (Cameron & Gaynor, 2014) at MfeI and XbaI sites. This recombines the gene at one of the 16S rRNA loci. This plasmid was electroporated into the *fqrB* mutant and colonies selected on Columbia blood agar plates plus kanamycin and apramycin.

4.3 | Overproduction and purification of proteins

The *fqrB*, *fldA*, and *nrdB* genes were cloned between the NdeI and XhoI sites of the pET21a vector (Novagen) such that a 6-his tag was attached in-frame to the C-terminus of the cognate proteins. The primers used are shown in Table 2. Each plasmid was transformed into *E. coli* BL21(DE3), grown in 1- to 5-L batches of LB media (plus carbenicillin 50 μg/ml) at 37°C to an OD 600 nm of 0.5, then protein production induced by 0.4-mM isopropyl-thiogalactoside (IPTG) for up to 3 (FldA), 5 (FqrB), or 6 hr (NrdB). Cells were harvested by centrifugation (10,000*g*, 10 min, 4°C), resuspended in binding buffer (20-mM sodium phosphate buffer pH 7.6, 0.5-M NaCl, 20-mM imidazole plus one Protease Inhibitor Mini Tablet [Pierce; Thermo Fisher Ltd, UK] per 20 ml), 10 units ml^{-1} DNAse I added (from bovine pancreas; Sigma Aldrich) and the cells disrupted by French Press (SLM Aminco) followed by centrifugation (15,500*g*, 10 min, 4°C) to remove debris. The supernatants were filtered (0.45 μm pore size) and pumped onto a 5 ml-HisTrap HP column (GE healthcare, UK) pre-equilibrated with binding buffer, connected to an AKTA Prime Protein Purification System. Proteins were eluted with a linear gradient of elution buffer (20-mM sodium phosphate buffer pH 7.6, 0.5-M NaCl, 0.5-M imidazole). For FldA and FqrB, further purification using HIC was performed using a 5-ml phenyl sepharose HIC column (GE healthcare, UK), with proteins bound in 50-mM Tris-HCl buffer pH 7.5 + 1.5 M ammonium sulfate and eluted with a linear

TABLE 2 Primers used in this work

Primer sequence 5′–3′	
FQRB_ISA_F1F	<u>GAGCTCGGTACCCGGGGATCCTCTAGAGTC</u>CATTTGTAAATTTTGCTTCA
FQRB_ISA_F1KR	<u>AAGCTGTCAAACATGAGAACCAAGGAGAAT</u>GACCTGCACCTACTACAATT
FQRB_ISA_F2KF	<u>GAATTGTTTTAGTACCTAGCCAAGGTGTGC</u>AGCAAGTATAGTTACAGGGTTA
FQRB_ISA_F2R	<u>AGAATACTCAAGCTTGCATGCCTGCAGGTC</u>AATACTCCAAAATTCCGAT
FQRB_COMP_F	ACAC**CAATTG**CATCTAACAAAAGCCTATCTTT
FQRB_COMP_R	ACAC*TCTAGA*TTATTTTGCATATGAATTTTCTAG
FLDA_OE_F	TATATT**<u>CATATG</u>**TCAGTAGCAGTAATCTATGGTAGT
FLDA_OE_R	ATTTAT*CTCGAG*AGCAAAATAAGGTTTGATTT
FQRB_OE_F	TATATT**<u>CATATG</u>**AAAAAAATAGATTTAATTGTAGTAGG
FQRB_OE_R	ATTTAT*CTCGAG*AAGCACAGAAAGAATTTTCA
NRDB_OE_F	TATATT**<u>CATATG</u>**CAAAGAAAAAGAATTTACAATC
NRDB_OE_R	ATTTAT*CTCGAG***GAAGTCATCAAAGCTTATACTACC**
KAN_F	ATTCTCCTTGGTTCTCATGTTTGACAGCTTAT
KAN_R	GCACACCTTGGCTAGGTACTAAAACAATTC

Note: Underlined bases are adaptor regions corresponding to the pGEM3zf vector (ISA F and R primers) or to the kanamycin resistance cassette (ISA KR and KF primers). COMP primers were used for complementation in the pRRA vector (MfeI site in bold; XbaI site in italics) and OE primers for overexpression in pET21a (NdeI sites underlined in bold; XhoI sites underlined in italics).

gradient of 50-mM Tris-HCl buffer pH 7.5. After purification, proteins were buffer exchanged into 50-mM Tris-HCl pH 7.5 using Vivaspin spin columns (Sartorius Stedim) with a molecular weight cut-off of at least 50% smaller than the protein size. Protein purity was assessed by SDS-PAGE.

4.4 | Mass spectrometry of NrdB

The two bands seen on SDS-PAGE gels of purified NrdB were cut out, divided into small pieces and de-stained in 500 μl acetonitrile/ammonium bicarbonate buffer (a 1:1 mixture of acetonitrile and 100-mM ammonium bicarbonate, pH 8.0). The supernatant was removed, and the gel pieces were washed thrice with the same buffer then dehydrated with 500-μl acetonitrile for 10 min. Two hundred microliters of 50-mM Tris(2-carboxyethyl)phosphine (TCEP) in 100-mM ammonium bicarbonate buffer pH 8.0 was added to reduce cysteines, with incubation for 20 min at 70°C. The supernatant was discarded and cysteines acetylated with 200 μl of 50-mM iodoacetamide in ammonium bicarbonate buffer. Gel pieces were then washed and dehydrated as above. For trypsin digestion, gel pieces were incubated in 200 μl of 1-ng/μl trypsin (Thermo Fisher Scientific) in ammonium bicarbonate buffer overnight at 37°C. One hundred microliters of acetonitrile was added the next day, and gel pieces were incubated for 15 min at 37°C. The digested peptides released in the supernatant were collected in a separate tube. Fifty microliters of 0.5% v/v formic acid was added to the gel pieces, and after 15 min, 100 μl of acetonitrile was added and incubated for an additional 15 min. The supernatant was transferred to the collection tube and the extraction with formic acid and acetonitrile repeated. Finally, the combined supernatant was incubated with 100 μl of acetonitrile for 15 min, resulting a final volume of 700 μl of digested peptides, which were dried down using a SpeedVac concentrator. To analyze the peptides via HPLC-MS, the pellet was resuspended in 40 μl 0.5% v/v formic acid. Twenty microliters of peptide solution was transferred to vials and analyzed by the Biological Mass Spectrometry Facility at The University of Sheffield. HPLC was done at 45°C using a Dionex UltiMate 3,000 system (Thermo Fisher Scientific) equipped with an Acclaim™ PepMap™ 100 C18, 20 × 75-μm Trap column (3-μm diameter particles and 100-Å pore size) and an EASY-Spray™ C18, 150 × 50 μm (2-μm diameter particles and 100-Å pore size) analytical nanocolumn. Mobile phase A consisted of 0.1% v/v formic acid in water and mobile phase B consisted of 0.1% v/v formic acid in 80% v/v acetonitrile. The gradient was formed at a flow rate of 250 ml/min as follows: 0–5 min at 4% B, then two steps of linear increase; first 40% B for 40 min then 90% B for 50 min. An LTQ Orbitrap Elite (Thermo Fisher Scientific) hybrid ion trap-orbitrap mass spectrometer and an EASY-Spray source with an ion transfer capillary at 250°C and a voltage of 1.8 kV were used for MS analysis. MS survey scans in positive ion mode were acquired in the FT-orbitrap analyzer using an m/z window from 375 to 1,600, a resolution of 60,000, and an automatic gain control target setting of 1×10^6. Using collision-induced dissociation (CID), the 20 most intense precursor ions were selected for the acquisition of tandem mass spectra in the dual cell linear ion trap at normal scan rate. Charge states 1 + were not included for precursor selection. Normalized collision energy was set to 35%, activation time to 10 ms, isolation width to 2 m/z, and automatic gain control value was set to 1×10^4. Identification of peptides/proteins was performed by MaxQuant (Cox & Mann, 2008), searching with default parameters.

4.5 | Inductively coupled plasma mass spectrometry

Purifed NrdB samples were added to 1 ml concentrated HNO_3 (65% v/v), left in acid overnight, and then analyzed at the University of Sheffield ICP-MS facility.

4.6 | Optical spectroscopy

Mediated potentiometric titration monitored by electronic absorbance spectroscopy was performed by the method of Dutton et al., (1970) with minor modification. The reductant was sodium dithionite, and the oxidant was potassium ferricyanide. The sample contained 50 μM CjFldA in 10-mM potassium phosphate buffer, pH 7.0 with the following mediators each at 10 μM; diaminodurene (E_m + 240 mV), phenazine methosulphate (E_m + 80 mV), phenazine ethosulphate (E_m + 55 mV), juglone (E_m + 30 mV), duroquinone (E_m + 5 mV), menadione (E_m – 70 mV), anthraquinone 2,6-disulphonate (E_m – 184 mV), anthraquinone-2-sulphonate (E_m – 225 mV). Flavodoxin semiquinone was quantified from the absorbance at 610 nm using an extinction coefficient of 3,900 $M^{-1}\,cm^{-1}$ (Mayhew et al., 1969). The plot of semiquinone concentration versus sample potential was fitted to the equation describing two sequential one-electron transfers to a single site:

$$\text{Semiquinone population} = \frac{1}{\left(1 + \theta_1 + \theta_2^{-1}\right)}$$

where $\theta_i = \exp(39(E - E_i))$, E is the sample potential, and E_1 and E_2 are the reduction potentials for addition of the first and second electron, respectively. Equivalent experiments without flavodoxin showed there was negligible spectral change from the mediators at 610 nm for potentials where the semiquinone was observed.

4.7 | Protein film electrochemistry

Cyclic voltammetry was performed using a three-electrode cell configuration inside a Faraday Cage within a N_2-filled chamber (atmospheric oxygen < 5 ppm). The reference electrode was Ag/AgCl (saturated KCl) and the counter electrode a platinum wire. The working electrode was pyrolytic graphite with the edge plane exposed to sample. Preparation of the working electrode was essentially as described by Seagel et al. (2017). Firstly, the surface was polished with

0.3-μm Al_2O_3 as an aqueous slurry, sonicated, rinsed with Milli-Q water and dried with a tissue. Secondly, 5 μl of 10-mM didodecyldimethylammonium bromide (DDAB) in Milli-Q water was placed on the electrode surface, the electrode covered with a beaker and left to dry overnight at ambient temperature. Finally, the DDAB-coated working electrode was taken into the N_2-filled chamber and 5 μl of 200-μM flavodoxin (in 50-mM phosphate, 150-mM NaCl, and pH 7.5) deposited on the surface. After 20 min, the working electrode was introduced to the electrochemical cell, which contained an aqueous solution of 50-mM potassium phosphate, pH 7. Cyclic voltammetry was performed with a PGSTAT30 potentiostat (Metrohm Autolab) under the control of NOVA 1.11 software. Measured potentials were converted to values versus SHE by addition of 197 mV.

4.8 | EPR spectroscopy

All EPR spectra were measured on a Bruker EMX EPR spectrometer (X-band). A Bruker resonator ER 4122 (SP9703) and an Oxford Instruments liquid helium system were used to measure the low-temperature (10 K) EPR spectra. Wilmad SQ EPR tubes (Wilmad Glass, Buena, NJ, USA) with OD = 4.05 mm and ID = 3.1 mm were used. Aliquots (250 μl) of the samples were placed in the EPR tubes, frozen in methanol and kept on dry ice (~195 K). The EPR tubes were then transferred to liquid nitrogen (77 K) and stored there until the measurements on the EPR spectrometer. Instrument settings are given in the relevant figure legends. The spectra were acquired by Dr Dima Svistunenko at the Biomedical EPR Facility, University of Essex, UK.

4.9 | Enzyme assays

All spectrophotometric assays were conducted at 37°C in a Shimadzu UV-2401 spectrophotometer. The ability of pyruvate and 2-oxoglutarate to act as electron donors to FldA via the action of the POR and OOR enzymes was assayed using cell-free extracts (CFE) of *C. jejuni* prepared by sonication under anaerobic conditions as described previously, in the presence an oxygen-scavenging system consisting of glucose oxidase, glucose, and catalase (Kendall et al., 2014). CFE was added to nitrogen-sparged 100-mM Tris-HCl buffer pH 8, 2-mM $MgCl_2$, 0.2-mM Coenzyme A, 0.1-mM thiamine pyrophosphate, and 50-μM purifed FldA in stoppered anaerobic cuvettes. The reaction was started by injection of anaerobic pyruvate or 2-oxoglutarate to 5-mM final concentration. Reduction of the FMN of FldA was followed at 460 nm. The NAD(P)H oxidase activity of FqrB was assayed at 340 nm (ε= 6.22 mM^{-1} cm^{-1}) in oxygen saturated 50-mM Tris-HCl buffer pH 7.5 after addition of FqrB (1 μM final) and either NADPH or NADH (300 μM final) to start the reaction. The reduction of FldA by FqrB and NAD(P)H was measured at 460 nm (estimated ε of 12 mM^{-1} cm^{-1}; Mayhew & Tollin, 1992) in 50-mM Tris-HCl buffer pH 7.5, 50-μM FldA, 0.1-μM FqrB, and 150 μM either NADH or NADPH to start the reaction.

4.10 | Preparation of radical free NrdB and reconstitution with FqrB, FldA, and NrdB

Purified NrdB was treated with 1 mM HA for 30 min then repeatedly buffer exchanged into 50-mM Tris-HCl pH 7.5 until no HA could be detected. Residual HA was detected by reaction with 8-hydroxyquinoline to form green indooxime after heating, which absorbs at 710 nm (Lanvers et al., 2002). Reconstitution assays with radical free NrdB were done in 50 mM Tris-HCl buffer pH 7.5 with 50-μM NrdB, 50-μM FldA, 5-μM FqrB, and 1-mM NADPH. Where samples were to be monitored by EPR, the buffer was changed to 20-mM Tris-HCl pH 7.7 plus 50-mM L-arginine and 50-mM L-glutamate to enhance NrdB stability.

4.11 | Phylogenetic analysis

Protein sequences were obtained from Uniprot. Multiple sequence alignments were made with CLUSTAL Omega and phylogenetic rees were generated and analyzed in JALVIEW, using publicly available software at www.expasy.org.

AUTHOR CONTRIBUTIONS
Conception and design of study; DJK. Acquisition, analysis and interpretation of data; AA, LA, JS, JB, and DJK. Writing of the manuscript; DJK, JB, and AA.

DATA AVAILABILITY STATEMENT
The data that support the findings of this study are available in the supporting information of this article (Tables S1 and S2).

ORCID
David J. Kelly 🔟 https://orcid.org/0000-0002-0770-6845

REFERENCES
Barker, P.D., Hill, H.A.O., Sanghera, G.S., Eady, R.R. & Thorneley, R.N.F. (1988) The direct electrochemistry of flavodoxin from *Azotobacter chroococcum* at a graphite electrode promoted by aminoglycosides. *Biochemical Society Transactions*, 16, 959–960. Available from: https://doi.org/10.1042/bst0160959

Berggren, G., Duraffourg, N., Sahlin, M. & Sjöberg, B.M. (2014) Semiquinone-induced maturation of *Bacillus anthracis* ribonucleotide reductase by a

superoxide intermediate. *Journal of Biological Chemistry*, *289*, 31940–31949.Available from: https://doi.org/10.1074/jbc.M114.592535

Bottin, H. & Lagoutte, B. (1992) Ferredoxin and flavodoxin from the cyanobacterium *Synechocystis* sp PCC 6803. *Biochimica Et Biophysica Acta*, *1101*, 48–56.

Calderon-Gomez, L.I., Day, C.J., Hartley-Tassell, L.E., Wilson, J.C., Mendz, G.L. & Korolik, V. (2017) Identification of NuoX and NuoY ligand binding specificity in the *Campylobacter jejuni* complex I. *Journal of Bacteriology & Parasitology*, *8*, 307. Available from: https://doi.org/10.4172/2155-9597.1000307

Cameron, A. & Gaynor, E. (2014) Hygromycin B and apramycin antibiotic resistance cassettes for use in *Campylobacter jejuni*. *PLoS One*, *9*, e95084. Available from: https://doi.org/10.1371/journal.pone.0095084

Carlone, G.M. & Anet, F.A. (1983) Detection of menaquinone-6 and a novel methyl-substituted menaquinone-6 in *Campylobacter jejuni* and *Campylobacter fetus* subsp. *fetus*. *Journal of General Microbiology*, *129*, 3385–3393.

Corrado, M.E., Zanetti, G. & Mayhew, S.G. (1996) The redox potentials of flavodoxin from *Desulfovibrio vulgaris* and ferredoxin-NADP+ reductase from *Spinacia oleracea* and their complexes. *Biochemical Society Transactions*, *24*, 28S. Available from: https://doi.org/10.1042/bst024028s

Cotruvo, J.A. Jr & Stubbe, J. (2008) NrdI, a flavodoxin involved in maintenance of the diferric-tyrosyl radical cofactor in *Escherichia coli* class 1b ribonucleotide reductase. *Proceedings of the National Academy of Sciences*, *105*, 14383–14388.

Cox, J. & Mann, M. (2008) MaxQuant enables high peptide identification rates, individualized p.p.b.-range mass accuracies and proteome-wide protein quantification. *Nature Biotechnology*, *26*, 1367–1372. Available from: https://doi.org/10.1038/nbt.1511

Dutton, P.L., Wilson, D.F. & Lee, C.P. (1970) Oxidation-reduction potentials of cytochromes in mitochondria. *Biochemistry*, *9*, 5077–5082.

Gaballa, A., Newton, G.L., Antelmann, H., Parsonage, D., Upton, H., Rawat, M. et al (2010) Biosynthesis and functions of bacillithiol, a major low-molecular-weight thiol in Bacilli. *Proceedings of the National Academy of Sciences*, *107*, 6482–6486.Available from: https://doi.org/10.1073/pnas.1000928107

Gibson, D.G., Young, L., Chuang, R.Y., Venter, J.C., Hutchison, C.A. 3rd & Smith, H.O. (2009) Enzymatic assembly of DNA molecules up to several hundred kilobases. *Nature Methods*, *6*, 343–345.Available from: https://doi.org/10.1038/nmeth.1318

Gudim, I., Hammerstad, M., Lofstad, M. & Hersleth, H.P. (2018) The characterization of different flavodoxin reductase-flavodoxin (FNR-Fld) interactions reveals an efficient FNR-Fld redox pair and identifies a novel FNR subclass. *Biochemistry*, *57*, 5427–5436.Available from: https://doi.org/10.1021/acs.biochem.8b00674

Haldenby, S., Bronowski, C., Nelson, C., Kenny, J., Martinez-Rodriguez, C., Chaudhuri, R. et al (2000) Increasing prevalence of a fluoroquinolone resistance mutation amongst *Campylobacter jejuni* isolates from four human infectious intestinal disease studies in the United Kingdom. *PLoS One*, *15*, e0227535.

Heering, H.A. & Hagen, W.R. (1996) Complex electrochemistry of flavodoxin at carbon-based electrodes: Results from a combination of direct electron transfer, flavin-mediated electron transfer and comproportionation. *Journal of Electroanalytical Chemistry*, *404*, 249–260. Available from: https://doi.org/10.1016/0022-0728(95)04248-2

Hein, S., von Irmer, J., Gallei, M., Meusinger, R. & Simon, J. (2018) Two dedicated class C radical S-adenosylmethionine methyltransferases concertedly catalyse the synthesis of 7,8-dimethylmenaquinone. *Biochimica Et Biophysica Acta—Bioenergetics*, *1859*, 300–308. Available from: https://doi.org/10.1016/j.bbabio.2018.01.010

Heuston, S., Begley, M., Gahan, C.G.M. & Hill, C. (2012) Isoprenoid biosynthesis in bacterial pathogens. *Microbiology*, *158*, 1389–1401. Available from: https://doi.org/10.1099/mic.0.051599-0

Hofer, A., Crona, M., Logan, D.T. & Sjöberg, B.M. (2012) DNA building blocks: Keeping control of manufacture. *Critical Reviews in Biochemistry and Molecular Biology*, *47*, 50–63.Available from: https://doi.org/10.3109/10409238.2011.630372

Hoganson, C.W. & Babcock, G.T. (1992) Protein-tyrosyl radical interactions in photosystem II studied by electron spin resonance and electron nuclear double resonance spectroscopy: Comparison with ribonucleotide reductase and in vitro tyrosine. *Biochemistry*, *31*, 11874–11880.Available from: https://doi.org/10.1021/bi00162a028

Hughes, N.J., Clayton, C.L., Chalk, P.A. & Kelly, D.J. (1998) *Helicobacter pylori porCDAB* and *oorDABC* genes encode distinct pyruvate: flavodoxin and 2-oxoglutarate: acceptor oxidoreductases which mediate electron transport to NADP. *Journal of Bacteriology*, *180*, 1119–1128. Available from: https://doi.org/10.1128/JB.180.5.1119-1128.1998

Johansson, R., Torrents, E., Lundin, D., Sprenger, J., Sahlin, M., Sjöberg, B.M. & et al (2010) High-resolution crystal structures of the flavoprotein NrdI in oxidized and reduced states—An unusual flavodoxin. Structural Biology. *FEBS Journal*, *277*, 4265–4277.Available from: https://doi.org/10.1111/j.1742-4658.2010.07815.x

Juhnke, H.D., Hiltscher, H., Nasiri, H.R., Schwalbe, H. & Lancaster, C.R. (2009) Production, characterization and determination of the real catalytic properties of the putative 'succinate dehydrogenase' from *Wolinella succinogenes*. *Molecular Microbiology*, *71*, 1088–1101.

Kendall, J.J., Barrero-Tobon, A.M., Hendrixson, D.R. & Kelly, D.J. (2014) Hemerythrins in the microaerophilic bacterium *Campylobacter jejuni* help protect key iron-sulphur cluster enzymes from oxidative damage. *Environmental Microbiology*, *16*, 1105–1121.

Konrad, A., Yarunova, E., Tinta, T., Piškur, J. & Liberles, D.A. (2012) The global distribution and evolution of deoxyribonucleoside kinases in bacteria. *Gene*, *492*, 117–120.Available from: https://doi.org/10.1016/j.gene.2011.10.039

Lanvers, C., Vieira Pinheiro, J.P., Hempel, G., Wuerthwein, G. & Boos, J. (2002) Analytical validation of a microplate reader-based method for the therapeutic drug monitoring of L-asparaginase in human serum. *Analytical Biochemistry*, *309*, 117–126.Available from: https://doi.org/10.1016/S0003-2697(02)00232-4

Lascelles, J. & Calder, K.M. (1985) Participation of cytochromes in some oxidation-reduction systems in *Campylobacter fetus*. *Journal of Bacteriology*, *164*, 401–409.Available from: https://doi.org/10.1128/JB.164.1.401-409.1985

Liu, Y.W. & Kelly, D.J. (2015) Cytochrome *c* biogenesis in *Campylobacter jejuni* requires cytochrome c_6 (CccA; Cj1153) to maintain apocytochrome cysteine thiols in a reduced state for haem attachment. *Molecular Microbiology*, *96*, 1298–1317.

Lofstad, M., Gudim, I., Hammerstad, M., Røhr, Å.K. & Hersleth, H.P. (2016) Activation of the Class 1b ribonucleotide reductase by a flavodoxin reductase in *Bacillus cereus*. *Biochemistry*, *55*, 4998–5001.

Mayhew, S.G., Foust, G.P. & Massey, V. (1969) Oxidation-reduction potentials of flavodoxin from *Peptostreptococcus elsdenii*. *Journal of Biological Chemistry*, *244*, 803–810.

Mayhew, S.G. & Tollin, G. (1992) General properties of flavodoxins. In: Müller, F. (Ed.) *Chemistry and biochemistry of flavoenzymes*. *3*, CRC Press, pp. 389–426.

Mikheyeva, I.V., Thomas, J.M., Kolar, S.L., Corvaglia, A.R., Gaïa, N., Leo, S. et al (2019) YpdA, a putative bacillithiol disulfide reductase, contributes to cellular redox homeostasis and virulence in *Staphylococcus aureus*. *Molecular Microbiology*, *111*, 1039–1056.

Parkhill, J., Wren, B.W., Mungall, K., Ketley, J.M., Churcher, C., Basham, D. et al (2000) The genome sequence of the food-borne pathogen *Campylobacter jejuni* reveals hypervariable sequences. *Nature*, *403*, 665–668.Available from: https://doi.org/10.1038/35001088

Petersson, L., Gräslund, A., Ehrenberg, A., Sjöberg, B.M. & Reichard, P. (1980) The iron center in ribonucleotide reductase from *Escherichia coli*. *Journal of Biological Chemistry*, *255*, 6706–6712.Available from: https://doi.org/10.1016/S0021-9258(18)43628-9

Puan, K.J., Wang, H., Dairi, T., Kuzuyama, T. & Morita, C.T. (2005) *fldA* is an essential gene required in the 2-C-methyl-D-erythritol 4-phosphate pathway for isoprenoid biosynthesis. *FEBS Letters*, 579, 3802–3806.

Roca, I., Torrents, E., Sahlin, M., Gibert, I. & Sjöberg, B.M. (2008) NrdI essentiality for class 1b ribonucleotide reduction in *Streptococcus pyogenes*. *Journal of Bacteriology*, 190, 4849–4858.

Rohdich, F., Zepeck, F., Adam, P., Hecht, S., Kaiser, J., Laupitz, R. et al (2003) The deoxyxylulose phosphate pathway of isoprenoid biosynthesis: Studies on the mechanisms of the reactions catalyzed by IspG and IspH protein. *Proceedings of the National Academy of Sciences*, 100, 1586–1591. Available from: https://doi.org/10.1073/pnas.0337742100

Rusling, J.F. (1998) Enzyme bioelectrochemistry in cast biomembrane-like films. *Accounts of Chemical Research*, 31, 363–369. Available from: https://doi.org/10.1021/ar970254y

Sahlin, M., Petersson, L., Gräslund, A., Ehrenberg, A., Sjöberg, B.M. & Thelander, L. (1987) Magnetic interaction between the tyrosyl free radical and the antiferromagnetically coupled iron center in ribonucleotide reductase. *Biochemistry*, 26, 5541–5548. Available from: https://doi.org/10.1021/bi00391a049

Salillas, S. & Sancho, J. (2020) Flavodoxins as novel therapeutic targets against *Helicobacter pylori* and other gastric pathogens. *International Journal of Molecular Sciences*, 21, 1881. Available from: https://doi.org/10.3390/ijms21051881

Sancho, J. (2006) Flavodoxins: Sequence, folding, binding, function and beyond. *Cellular and Molecular Life Sciences*, 63, 855–864. Available from: https://doi.org/10.1007/s00018-005-5514-4

Sandrini, M.P., Clausen, A.R., Munch-Petersen, B. & Piskur, J. (2006) Thymidine kinase diversity in bacteria. *Nucleosides, Nucleotides & Nucleic Acids*, 25, 1153–1158. Available from: https://doi.org/10.1080/15257770600894469

Seagel, H.M., Spatzal, T., Hill, M.G., Udit, A.K. & Rees, D.C. (2017) Electrochemical and structural characterization of *Azotobacter vinelandii* flavodoxin II. *Protein Science*, 26, 1984–1993.

Sellars, M.J., Hall, S.J. & Kelly, D.J. (2002) Growth of *Campylobacter jejuni* supported by respiration of fumarate, nitrate, nitrite, trimethylamine-N-oxide, or dimethyl sulfoxide requires oxygen. *Journal of Bacteriology*, 184, 4187–4196. Available from: https://doi.org/10.1128/JB.184.15.4187-4196.2002

Sheppard, S.K., Dallas, J.F., Strachan, N.J.C., MacRae, M., McCarthy, N.D., Wilson, D.J. et al (2009) *Campylobacter* genotyping to determine the source of human infection. *Clinical Infectious Diseases*, 8, 1072–1078.

Smith, M.A., Finel, M., Korolik, V. & Mendz, G.L. (2000) Characteristics of the aerobic respiratory chains of the microaerophiles *Campylobacter jejuni* and *Helicobacter pylori*. *Archives of Microbiology*, 174, 1–10. Available from: https://doi.org/10.1007/s002030000174

St Maurice, M., Cremades, N., Croxen, M.A., Sisson, G., Sancho, J. & Hoffman, P.S. (2007) Flavodoxin:quinone reductase (FqrB): A redox partner of pyruvate:ferredoxin oxidoreductase that reversibly couples pyruvate oxidation to NADPH production in *Helicobacter pylori*

and *Campylobacter jejuni*. *Journal of Bacteriology*, 189, 4764–4773. Available from: https://doi.org/10.1128/JB.00287-07

Stubbe, J. & Cotruvo, J.A. Jr (2011) Control of metallation and active cofactor assembly in the class 1a and 1b ribonucleotide reductases: Diiron or dimanganese? *Current Opinion in Chemical Biology*, 15, 284–290.

Taylor, A.J. & Kelly, D.J. (2019) The function, biogenesis and regulation of the electron transport chains in *Campylobacter jejuni*: New insights into the bioenergetics of a major food-borne pathogen. *Advances in Microbial Physiology*, 74, 239–329.

Torrents, E. (2014) Ribonucleotide reductases: Essential enzymes for bacterial life. *Frontiers in Cellular and Infection Microbiology*, 4, 52. Available from: https://doi.org/10.3389/fcimb.2014.00052

van der Stel, A.X., Boogerd, F.C., Huynh, S., Parker, C.T., van Dijk, L., van Putten, J.P.M. et al (2017) Generation of the membrane potential and its impact on the motility, ATP production and growth in *Campylobacter jejuni*. *Molecular Microbiology*, 105, 637–651.

van Vliet, A.H., Wooldridge, K.G. & Ketley, J.M. (1998) Iron-responsive gene regulation in a *Campylobacter jejuni* fur Mutant. *Journal of Bacteriology*, 180(20), 5291–5298. Available from: https://doi.org/10.1128/JB.180.20.5291-5298.1998

Wang, M., Feng, W.Y., Zhao, Y.L. & Chai, Z.F. (2010) ICP-MS-based strategies for protein quantification. *Mass Spectrometry Reviews*, 29, 326–438. Available from: https://doi.org/10.1002/mas.20241

Weerakoon, D.R. & Olson, J.W. (2008) The *Campylobacter jejuni* NADH:Ubiquinone oxidoreductase (complex I) utilizes flavodoxin rather than NADH. *Journal of Bacteriology*, 190, 915–925. Available from: https://doi.org/10.1128/JB.01647-07

Wu, C.H., Jiang, W., Krebs, C. & Stubbe, J. (2007) YfaE, a ferredoxin involved in diferric-tyrosyl radical maintenance in *Escherichia coli* ribonucleotide reductase. *Biochemistry*, 46, 11577–11588.

Yahara, K., Méric, G., Taylor, A.J., de Vries, S.P.W., Murray, S., Pascoe, B. et al (2017) Genome-wide association of functional traits linked with *Campylobacter jejuni* survival from farm to fork. *Environmental Microbiology*, 19, 361–380.

SUPPORTING INFORMATION

Additional Supporting Information may be found online in the Supporting Information section.